Environ Earth Sci (2015) 73:4659–4670
DOI 10.1007/s12665-014-3751-2

ORIGINAL ARTICLE

The distance decay of similarity in climate variation and vegetation dynamics

Zhiqiang Zhao · Shuangcheng Li · Jianguo Liu · Jian Peng · Yanglin Wang

Received: 3 January 2014 / Accepted: 29 September 2014 / Published online: 15 October 2014

Abstract The negative relationship between similarity and distance has been revealed in many subjects in geography and ecology fields. This study aimed to illustrate the strength of the distance-decay relationship in variation of climate and vegetation, and to quantify the relationship. Solving this problem could help to test some model specifications based on the climate and vegetation time series on sample sites, to determine the distance function in the spatial interpolation technique for meteorological factors and vegetation dynamics, and to use the distance-decay perspective as a quantitative technique to adapt strategies for future climate change and vegetation dynamics. To achieve the study goal, we quantified variation similarity using mutual information (MI), which measured the dependence between two variables or time series. We carried out a distance-decay analysis of climate and NDVI variation similarities, assessed by the MI against the log-transformed geographical distances between meteorological stations. The results suggest that all station pairs shared some similarity in the processes of climate variation and vegetation dynamics, and the MI values showed a gradual decrease with the increase of distance. In addition, temperature, precipitation, and NDVI time series had different MI value ranges and distance-decay ratios due to various influential factors. The logarithmic distance-decay relationships are of potential usefulness to the study of community similarity and the neutral theory of biogeography. Our research provides an approach for analyzing spatial patterns in relation to dependence and synchronization that may inform future studies aiming to understand the distribution and spatial relationship of climate and vegetation changes.

Keywords Distance decay · Spatial pattern · Mutual information · Climate · NDVI · China

Z. Zhao (✉) · S. Li · J. Peng · Y. Wang (✉)
Laboratory for Earth Surface Processes, Ministry of Education, College of Urban and Environmental Sciences, Peking University, Beijing 100871, China
e-mail: zqzhao0324@gmail.com

Y. Wang
e-mail: ylwang@urban.pku.edu.cn

J. Liu
Department of Fisheries and Wildlife, Center for Systems Integration and Sustainability, Michigan State University, East Lansing, MI 48823, USA

Introduction

One of the most important fundamental concepts of geography is distance decay, which was once called the "First Law of Geography": Everything is related to everything else, but near things are more related than distant things (Tobler 1970; Sui 2004). This law indicated that the similarity between two observations often decreases or decays as the distance between them increases (Nekola and White 1999). The early study of distance decay raised great interest among researchers in spatial autocorrelation, and led eventually to the field of geostatistics (Cressie 1993; Nekola and White 1999). In recent years, spatial dependency, which indicates the co-variation of properties within geographic space, has become one of the most important terms in geography (Prates-Clark et al. 2008; Chen and Henebry 2010; Martinez et al. 2010; Viedma et al. 2012).

The negative relationship between similarity and distance covers many subjects in the fields of geography and ecology and is related to some key theoretical issues such as what determines diversity, distribution, and abundance

of species, and the way in which analyses in ecology are performed (Bjorholm et al. 2008). In spatial biodiversity studies, distance decay describes how the similarity in species composition between two communities varies with the geographic distance that separates them (Morlon et al. 2008). Generally, studies illustrated that species turnover produces a decrease of similarity with distance along spatial environmental gradients (Whittaker 1975; Cody 1975; Baselga 2007; Soininen et al. 2007; Bjorholm et al. 2008; Astorga et al. 2011). In island biogeography, studies demonstrated a decrease in percent species saturation of oceanic or habitat islands as a function of their distance from a source pool of immigrants (Vuilleumier 1970; Kadmon and Pulliam 1993; Nekola and White 1999).

Nevertheless, few studies have extended the distance-decay relationships to the fields of climate variation and vegetation dynamics. Although several regional studies have qualitatively indicated that the similarity or correlation of the normalized difference vegetation index (NDVI) and precipitation time series decreases as distance increases (Walsh et al. 2001; Millward and Kraft 2004; Zhang et al. 2009; Costantini et al. 2012), only a limited number of studies have quantitatively discussed the distance-decay function, such as Domroes and Ranatunge (1993), Baigorria et al. (2007), Hofstra and New (2009), and Baigorria and Jones (2010). Previous studies were mainly concentrated on climate data of meteorological stations to interpolate climatic data of meteorological stations and to create gridded climate databases by investigating the distance-decay relationships. However, to our knowledge, no previous studies have been performed to assess and compare the distance-decay functions of vegetation dynamics and climatic factors time series.

Due to the high cost and difficulty of gathering data, many studies were point based but nevertheless more interested in a wide range of large-scale regional events. For instance, when using the tree-ring parameters to reconstruct historical climate variance and vegetation dynamic, Chen et al. (2012) analyzed whether the reconstruction series had common signals for large areas. Investigating the relationship between distance and the similarity of modern climate and vegetation time series through extrapolation based on distance-decay functions could contribute to solving the problem of generalizing historical, modern, and future climate change from sampling points to regional climatic variations. Also, it could help test various model specifications related to point-based databases to determine the distance function in a spatial interpolation technique for creating gridded meteorological elements and vegetation dynamics databases. Such an investigation could use the distance-decay perspective to create adaptive strategies for future global change based on the research material of a demonstration zone.

NDVI has been commonly used as an estimator of terrestrial vegetation dynamics and distributions, and many researchers have focused on the spatial and temporal correlations between NDVI values and climatic factors (Li et al. 2011; Zhao et al. 2014). In this study, we first quantify variation similarity by adopting the method of mutual information (MI), which measures the dependence between NDVI, temperature, and precipitation time series. Then the preliminary results are presented, which focus on the spatial patterns of MI and the distance-decay relationship. In addition, using multivariate analysis, we concerned whether there were coupled effects from climate variation similarity and geographic distances to explain the similarity of vegetation dynamics between meteorological stations. Finally, we conclude by discussing the implication of our results concerning studies of distribution and the spatial relationship of climate and vegetation change in geography.

Methods and materials

Methods

Mutual information

Various methods have been used to characterize the relationship between time-series data. Most commonly, the methods were based on regression and correlation analysis (Geerken et al. 2005; Brown et al. 2006; White et al. 2009; Lhermitte et al. 2011), and some adopted transformation approaches, such as principal component analysis (Gurgel and Ferreira 2003; Lobo and Maisongrande 2008) and Fourier transform (Lhermitte et al. 2008). Among these measurements of independence between random variables, mutual information (MI) is singled out by its information-theoretic background (Cover and Thomas 2006). Previous studies generally were based on correlation analysis to describe the dependence structure between climate and vegetation time series, and it was incomplete. In contrast to linear correlation coefficient, MI is sensitive also to dependencies that do not manifest themselves in covariance (Kraskov et al. 2004).

The definition of MI between two random variables is given by Shannon and Weaver (1949) and Cover and Thomas (2006). For a system X with a finite set of N possible states $\{x_1, x_2, \ldots, x_N\}$ and system Y with a finite set of N possible states $\{y_1, y_2, \ldots, y_N\}$ the MI of X relative to Y, denoted $I(X; Y)$, is defined as

$$I(X;Y) = \sum_{i,j} P(x_i, y_j) \log \frac{P(x_i, y_j)}{P(x_i)P(y_j)} \quad (1)$$

where $P(x_i, y_j)$ is the joint probability distribution function of X and Y, and $P(x_i)$ and $P(y_j)$ are the marginal probability distribution functions of X and Y, respectively.

MI is useful for investigating the dependence between two variables. High MI between two variables indicates a large reduction in uncertainty; that is, one time series is non-randomly associated with the other. On the other side, low MI indicates a small reduction. MI is zero if and only if the two time series are statistically independent. Therefore, MI can be used as an indicator between two time series related to their degree of independence. We assume that the higher the MI is between two time series, the more similar the variations will be.

Geographical distance

In this study, geographical distance between meteorological stations was computed using formulas of spherical trigonometry on the sphere that best approximates earth's surface. The geographical distance is the arc length between any two points on the surface of the earth.

The distance between stations i and j can be given by:

$$D_{i,j} = R \times \arccos\left(\sin J_i \sin J_j + \cos W_i \cos W_j \cos \Delta W\right) \quad (2)$$

where J_i, W_i; J_j, W_j are the geographical latitude and longitude of two points, respectively, and ΔJ, ΔW their differences; then R is the radius of the earth ($R = 6{,}370$ km).

This distance is the shortest distance along the great circle that contains the two points. Due to the irregularity between the sphere and earth's surface, the possible error is 0.5 %.

Data sources

Meteorological data

Temperature and precipitation were selected to analyze the variations of climate. The data were obtained from the China Meteorological Administration (http://cdc.cma.gov.cn/). Among the 752 meteorological stations, 652 stations were selected due to the short historical records or missing observations in some stations. To match the length of NDVI series, the original daily temperature and precipitation data from 1 April 1998 to 31 December 2008 were aggregated into 10-day time series, which contained 387 data points each. The quality of climatic data was strictly controlled by verifying climatic range, weather singular value, and inner coherence.

Normalized difference vegetation index

NDVI has been widely used as an estimator of plant productivity (Davies et al. 2007; Evans et al. 2006; Kerr and Ostrovsky 2003) and an index for green cover monitoring (Maselli and Chiesi 2006; Myneni et al. 1998). It is computed as the ratio of two electromagnetic wavelengths (near infrared − red)/(near infrared + red). For this study, an NDVI time series of satellite observations at 1-km spatial and 10-day (dekads) temporal resolutions were used, covering the period from April 1998 to December 2008. The time series was produced by Vlaamse Instelling voor Technologisch Onderzoek (VITO) from the sensor VEGETATION on board the SPOT-4 satellite. A registered user can download the free SPOT-4 VEGETATION 10-day synthesis (called "VGT-S10") NDVI data via the VGT Website (http://free.vgt.vito.be/). VGT-S10 NDVI products were synthesized from S1 (1-day resolution) NDVI products using a maximum value composite algorithm (Jarlan et al. 2008).

NDVI values for each meteorological station were extracted in raster format from each VGT-S10 image using ArcGIS software. To reduce noise in an NDVI series, its values for a given station were derived and averaged within a 10-km buffer circle.

Analyses

By computing the MI value of NDVI, temperature, and precipitation time series between each meteorological station and the other 651 stations, three 652 × 652 matrices are constructed, respectively. Similarly, one matrix of distance with 652 meteorological stations was obtained. The MI and distance coefficients are symmetric ($MI_{i,j} = MI_{j,i}$, $d_{ij} = d_{ji}$). After removing the redundant values and the main diagonal, there are 212,226 (=652 × (652−1)/2) MI or distance values per matrix. Each matrix is unfolded into a vector of MI and distances, and the data were calculated as the correlation between the two vectors (Legendre and Legendre 1998; Lichstein 2007). For more detailed descriptions about the distance matrix and method, readers can refer to the references by Mantel (1967), Legendre and Legendre (1998), and Lichstein (2007).

According to climatic regionalization, eastern China shows a noticeable characteristic of latitudinal zonality, specifically recognized as a range from tropics through subtropics and warm temperate and temperate zones to cool temperate zones. Thus, in eastern China, we chose 40 stations, located between 115°E and 117°E, as a longitudinal sampling belt. Meanwhile, northern China shows clear longitudinal zonality as the distribution of continents and oceans shift from humid regions through sub-humid and semi-arid regions to arid regions. Therefore, 50 stations (39°N–41°N) were selected, forming a latitudinal sampling belt.

Limited by space, not all spatial patterns of MI and the distance-decay curves of the meteorological stations are presented in this paper. Four stations at the end of the two

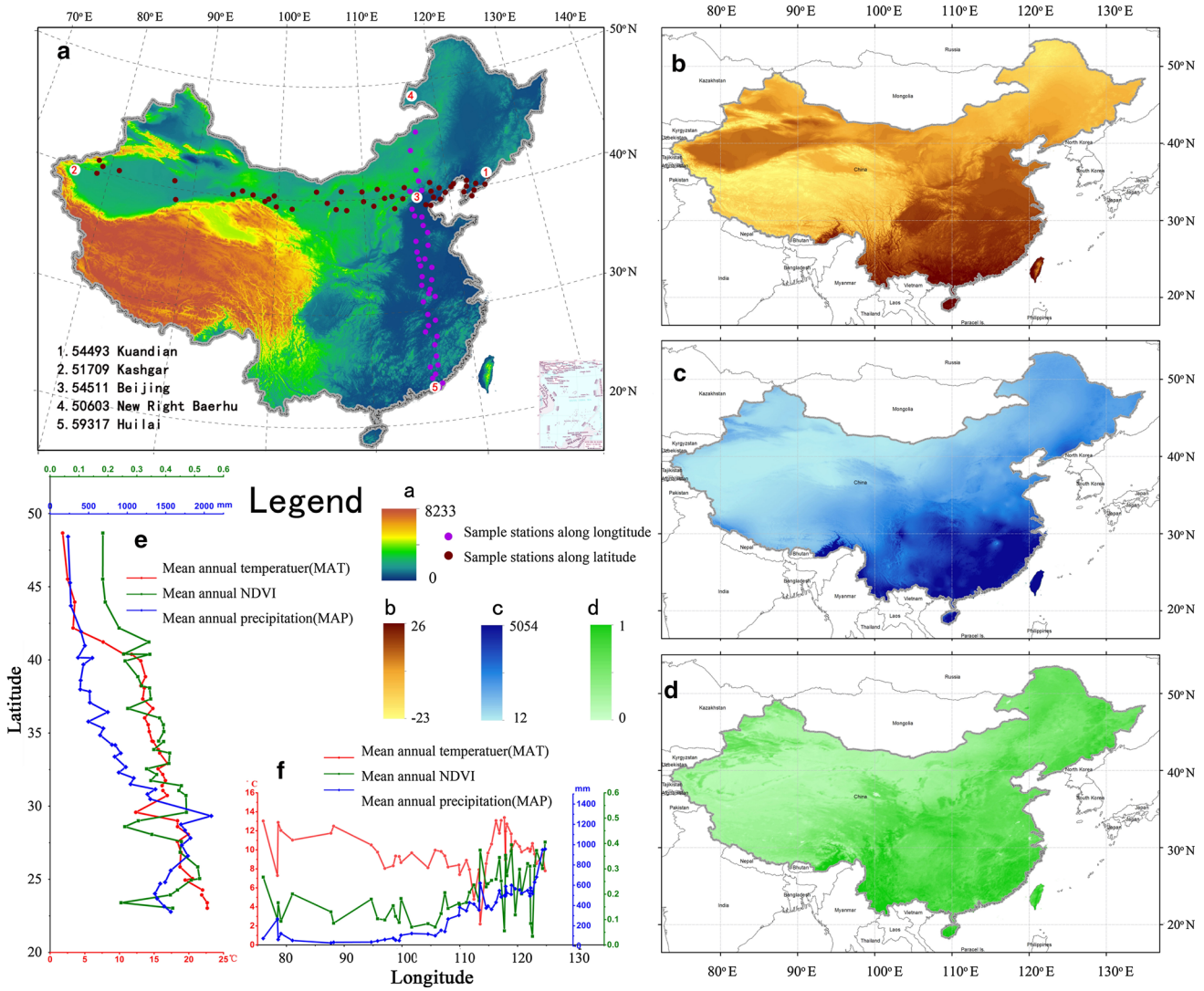

Fig. 1 **a** Topography of China, with location of 40 longitudinal sampling sites (*purple*), 50 latitudinal sampling sites (*brown*), and Beijing station and the endpoint meteorological stations (*1–5*) of the sampling belts used in this study; **b** mean annual temperature of China; **c** mean annual precipitation of China; **d** mean annual NDVI of China; **e** mean annual precipitation (*blue*), annual temperature (*red*), and annual NDVI (*green*) of 40 longitudinal sampling sites; **f** average annual precipitation (*blue*), annual temperature (*red*), and annual NDVI (*green*) of 50 latitudinal sampling sites

Table 1 Beijing station and the endpoint meteorological stations of the sampling belts

Station code	Name	Longitude	Latitude	Elevation (m)
54493	Kuandian	124.47°E	40.43°N	260
51709	Kashgar	75.59°E	39.28°N	1,288
54511	Beijing	116.17°E	39.56°N	54
50603	New Right Baerhu	116.49°E	48.40°N	554
59317	Huilai	116.18°E	23.02°N	13

sampling belts (Fig. 1a; Table 1) are regarded as examples to show the results, so the MI distance-decay curves could cover a large range of distance (from 100 km to 4,500 km) when doing regression analysis to reproduce distance-decay relationships. Meanwhile, to contrast the differences of distance-decay relationships of MI between longitude and latitude, we chose station 54511 (Fig. 1a; Table 1) among several stations located within both sampling belts.

In this study, the MI matrixes and distance matrix were computed in Matlab 2010a (The MathWorks Inc., Natick, MA, USA). MI of climate and vegetation variability

Table 2 The ranges of MI values across all stations

	NDVI	Precipitation	Temperature
Mean MI	0.413	0.157	1.251
Maximum MI	2.373	1.311	3.675
Minimum MI	0.017	0.011	0.004

between meteorological stations was calculated according to formula (1).

We carried out a distance-decay analysis of climate and NDVI variation similarities, assessed by the MI against the log-transformed geographical distance between meteorological stations in kilometers.

$$\mathrm{MI}_{i,j} = a + b \times \log D_{i,j} \quad (3)$$

where $D_{i,j}$ is the distance and $\mathrm{MI}_{i,j}$ is the mutual information of the time series from the two stations i and j, a is the intercept, and b is the slope.

Additionally, the correlations between vegetation dynamics similarity, climate dynamics similarity, and distance were, respectively, analyzed by Pearson Correlation Coefficient and multiple liner regression analysis.

The fitting models and Pearson correlation coefficient analysis were performed with the use of R, version 3.0.1 (www.r-project.org). Statistical hypothesis and significance were verified by F test and t test.

Results

Overall mutual information of the variations

By computing the MI value of NDVI, temperature, and precipitation time series between each meteorological station and the other 651 stations, 212,226 MI data were obtained, respectively. The MI values of the NDVI series ranged from 0.017 to 2.373, and the range of MI values of the precipitation series was $0.011 \sim 1.311$, while the temperature series ranged from 0.004 to 3.675 (Table 2). The minimum and maximum MI of NDVI, precipitation, and temperature series between the selected station and the rest of the 651 meteorological stations are shown in Table 3.

As shown in Tables 2 and 3, the minimum MI was quite close to zero, but not equal to zero. By the definition of MI, the results suggested that there were no fully statistically independent NDVI, precipitation, and temperature time series between any two stations; that is, all station pairs shared some similarity in the processes of climate variation and vegetation dynamics. The results conformed to the first statement in the "First Law of Geography"—"everything is related to everything else," which denotes explicit spatial dependence (Sui 2004). This result is helpful in understanding the synchronism in climate change and teleconnections, the climate dynamics and anomalies being correlated over large distances.

Spatial patterns of the mutual information

The spatial patterns of MI of the NDVI, temperature, and precipitation series between each selected station and the rest of the 651 meteorological stations exhibited significant regional differentiations (Fig. 2). Overall, the highest values of MI were observed near selected stations; in contrast, the lowest value areas were far away from the selected stations. Compared to NDVI and precipitation, the temperature series had obviously regular MI patterns. Meanwhile, MI of precipitation and NDVI series showed more multifaceted patterns, some characteristic contour details besides global regularity.

The figures of NDVI series suggested clear north–south differences, and in the Tsaidam Basin, a desert region, the MI values also showed a low value area of basin shape. Among the MI patterns of NDVI series, the pattern of station 59317 [Fig. 2 (1e)] displayed the largest differences between the other four figures [Fig. 2 (1a–1d)]. Besides, similar differences could be found in MI patterns of temperature and precipitation series. MI of precipitation series showed relatively smooth change, and the higher value areas are in a very small range. Especially, the high value areas are confined to small distances [Fig. 2 (3b)], which revealed the MI pattern between station 51709, located in

Table 3 The ranges of MI values of the selected stations

	NDVI			Precipitation			Temperature		
	MI_mean	MI_min	MI_max	MI_mean	MI_min	MI_max	MI_mean	MI_min	MI_max
50603	0.492	0.034	1.302	0.138	0.027	0.723	1.318	0.025	3.015
51709	0.478	0.053	1.421	0.064	0.015	0.307	1.270	0.027	2.698
54493	0.542	0.036	1.871	0.180	0.030	0.963	1.412	0.028	2.849
54511	0.469	0.037	1.271	0.179	0.032	0.664	1.409	0.026	2.820
59317	0.250	0.055	1.003	0.148	0.033	0.933	1.071	0.038	3.049

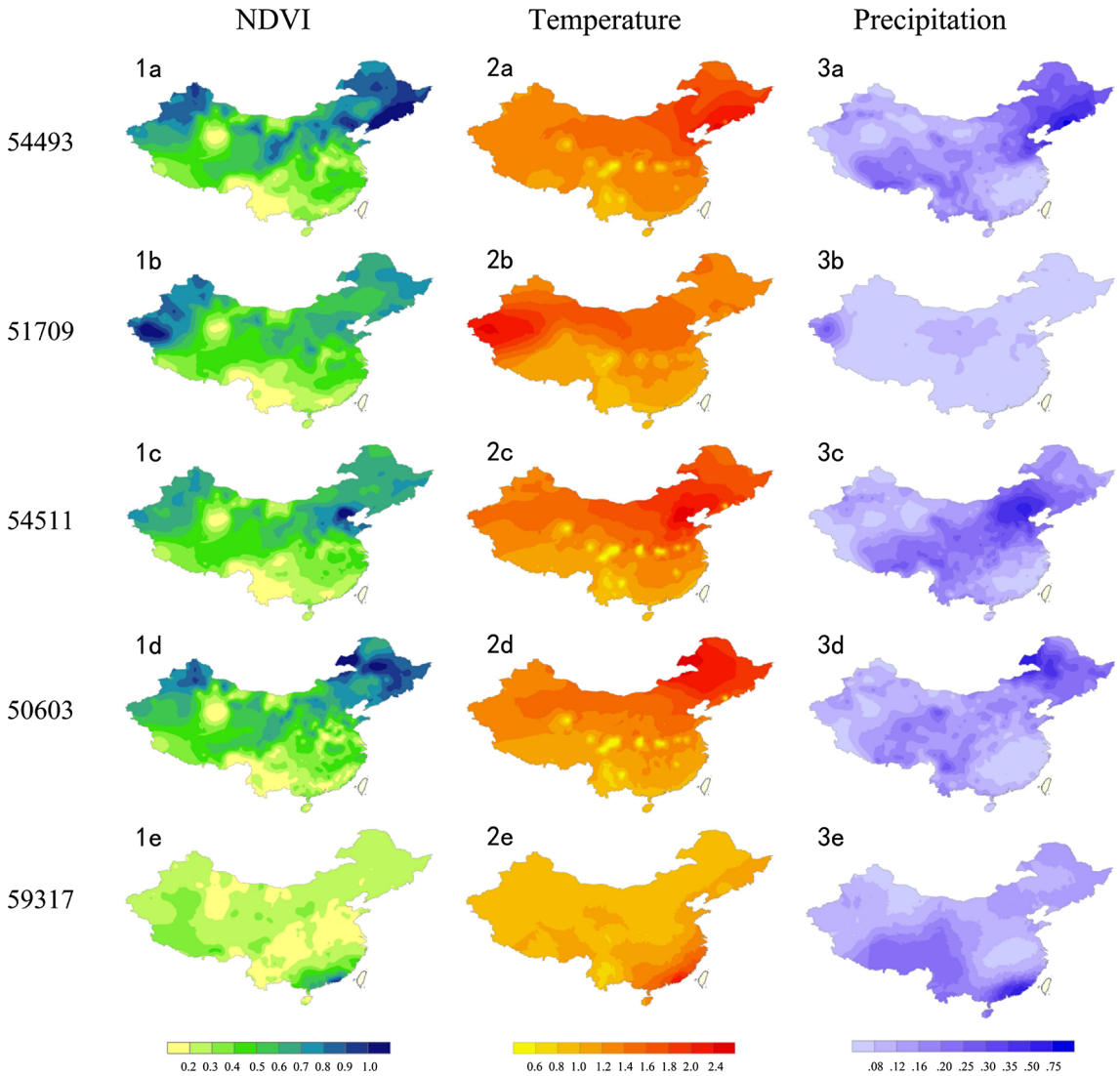

Fig. 2 Spatial patterns of MI of NDVI, precipitation, and temperature series between each selected station and the other 651 stations; **1a**, **2a**, and **3a,** respectively, indicate the kriging interpolation results of MI of NDVI, temperature, and precipitation series at station 54493; **1b**, **2b**, and **3b** for station 51709; **1c**, **2c**, and **3c** for station 54511; **1d**, **2d**, and **3d** for station 50603; and **1e**, **2e**, and **3e** for station 59317

Tarim Basin, and other stations. MI patterns of temperature series in Fig. 2a–e indicated significantly lower value centers along the important dividing line between north and south China, including Sichuan Basin, Qinling Mountains, and Huai River. Moreover, this line approximates the 0 °C January isotherm and the 800-mm isohyet in China.

Producing distance-decay relationships

Using distance between each two meteorological stations as the independent variable and MI of the time series from the two stations as the dependent variable, we did a regression analysis to reproduce distance-decay relationships.

As presented in Fig. 3, which displayed the whole 212,226 data points from the 652 meteorological stations, the MI values decreased with distance. The distance-decay pattern showed an initial high rate of change, smoothing its slope around MI values of 1.5, 0.5, and 0.25 for temperature, NDVI, and precipitation time series, respectively. After 1,500 km, the MI constantly decayed at slower values (Fig. 3). According to the decline features, we carried out a distance-decay analysis of climate and NDVI variation similarities, assessed by the MI against the log-transformed geographical distance between meteorological stations in kilometers. The results showed that MI was negative and significantly correlated with log-transformed geographical distances for precipitation (Intercept $= 0.830$, Slope $= -0.093$, $R^2 = 0.372$, $P < 0.001$ for F test) and temperature (Intercept $= 3.541$, Slope $= -0.316$, $R^2 = 0.306$, $P < 0.001$ for F test), however, almost

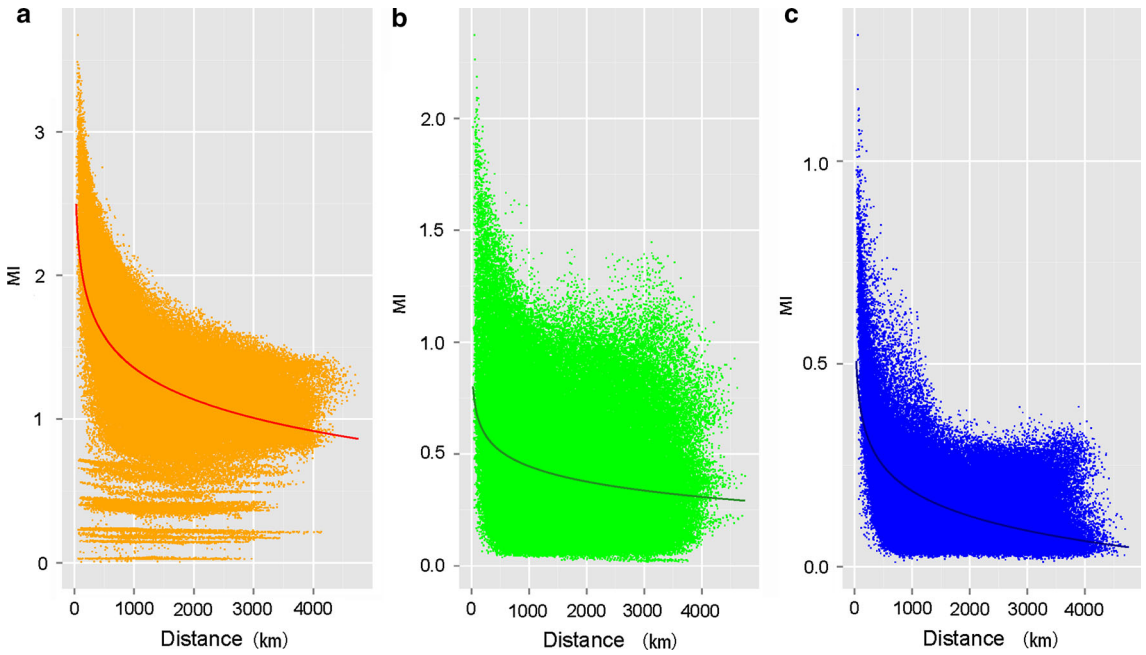

Fig. 3 Distance-decay analysis of MI for temperature, NDVI, and precipitation time series between 652 meteorological stations. The *lines* represent the log-transformed geographic distance model, **a** indicates a distance-decay analysis of MI for temperature time series; **b** NDVI; **c** precipitation

no logarithmic correlation for NDVI time series (Intercept = 1.105, Slope = −0.096, $R^2 = 0.062$, $P < 0.001$ for F test).

Since the study area has vast terrain and diverse climate, with significant latitudinal and longitudinal zonality, the distance-decay model will change along with the different regions and sampling belts. The five selected stations of the two sampling belts (Fig. 1a; Table 1) are regarded as examples to show the differences between longitude and latitude. As shown in Fig. 4 and Table 4, the MI distance-decay curves were generally similar to each other, but had different details. Among the three indexes, the temperature series produced the highest initial MI and regression slopes, the NDVI series produced lower initial MI and regression slopes, and the precipitation series produced the lowest initial MI and regression slopes. However, the models of NDVI series had lower R^2 values than temperature and precipitation series models. The vegetation dynamics were closely coupled with climatic fluctuations and land use. Consequently, the spatial patterns of NDVI time series were more complicated than those of climate time series, especially in inhomogeneous regions. Therefore, the distance-decay relationships of NDVI series were not as significant as the relationships of temperature and precipitation series.

With the 200-mm isohyet as boundaries, eastern China has a monsoon climate while western China has a continental climate. The latitudinal sampling belt was located within the eastern monsoon climate, where latitudinal zonality was quite obvious and continuous, thus the pattern of distance decay was relatively evident. However, the longitudinal sampling belt crossed two climate regions, and longitudinal zonality was interrupted by undulating terrain and other factors (Fig. 1a, e, and f), hence the pattern of distance decay in this belt was not significant. Moreover, because there are fewer climate stations in western China, the sampling points in the longitudinal belt were sparse and unevenly distributed. Therefore, the results showed that fitness (R^2) of the models along the latitude belt were much lower than those along the longitude belt, especially for the NDVI time series. As presented in Fig. 3 and Table 4, for station 54511, the distance-decay curve of the NDVI time series was more significant at the longitudinal sampling belt ($R^2 = 0.694$) than at the latitudinal sampling belt ($R^2 = 0.408$). Furthermore, for the other two latitudinal stations in Fig. 4 and Table 4, the logarithmic regression models of the NDVI time series had either a low correlation coefficient ($R^2 = 0.408$, 54493) or no logarithmic correlation between MI and distance at the 95 % confidence level ($R^2 = 0.018$, 51709). Besides the difference between the monsoon climate and continental climate, due to the uneven terrain, the distance-decay relationship was not clear along the latitudinal sampling belt, particularly the model at 51709 in the NDVI series (Fig. 4d; Table 4). Kashgar (51709), which is located at the edge of Taklimakan Desert, featured a desert climate and had very low

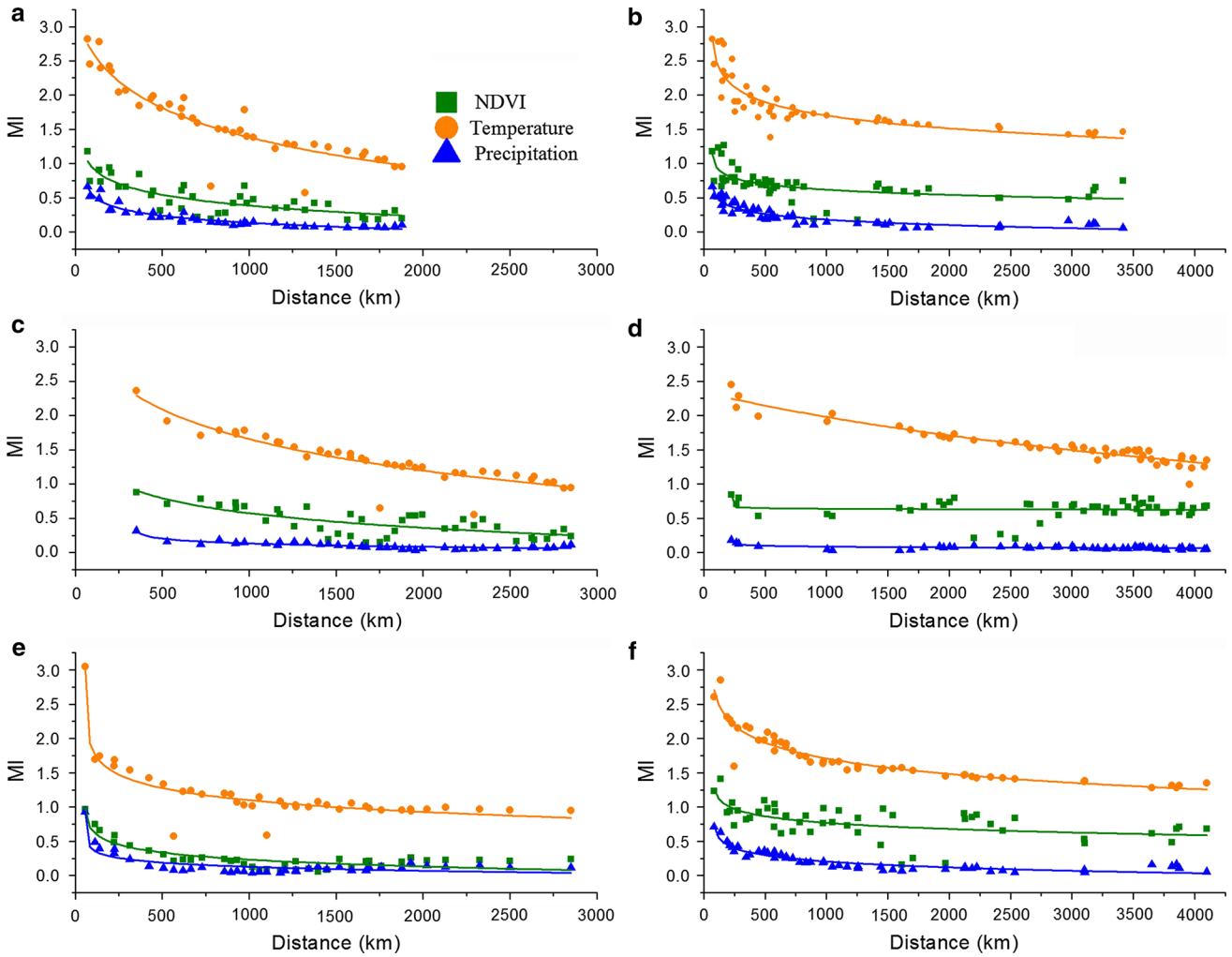

Fig. 4 Decrease in MI with geographic distance between meteorological stations. The *lines* indicate the logarithmic regressions, **a** indicates a distance-decay relationship along longitude at 54511; **b** along latitude at 54511; **c** along longitude at 50603; **d** along latitude at 51709; **e** along longitude at 59317; **f** along latitude at 54493

Table 4 Regression parameters for the relationship between MI and geographic distance in datasets (confidence level of 95 %)

Long	Sets	Adj. R^2	In	Slope	Lat	Sets	Adj. R^2	In	Slope
54511 (a)	Temp	0.841	6.168	0.685	54511 (b)	Temp	0.755	3.489	0.261
	NDVI	0.694	1.929	0.224		NDVI	0.408	1.340	0.105
	Prec	0.904	1.090	0.139		Prec	0.840	0.939	0.111
50603 (c)	Temp	0.800	6.624	0.709	51709 (d)	Temp	0.904	10.661	1.065
	NDVI	0.531	2.659	0.303		NDVI	0.018	0.698	0.009
	Prec	0.758	0.480	0.053		Prec	0.537	0.174	0.013
59317 (e)	Temp	0.856	2.718	0.236	54493 (f)	Temp	0.880	3.867	0.314
	NDVI	0.775	1.197	0.141		NDVI	0.336	1.622	0.125
	Prec	0.807	0.692	0.082		Prec	0.872	1.019	0.119

Long the sites along longitude, *Lat* the sites along latitude, *Temp* temperature, *Prec* precipitation, *NDVI* normalized difference vegetation index, *Adj.* R^2 adjusted R^2, *In* intercept, *a–e* corresponding subplots in Fig. 3

NDVI values, very similar to the desert area in the east. However, in very similar latitudes, the alpine steppe in eastern Qinghai and southern Gansu had higher NDVI values. Then eastward, stations in the desert grassland and dry steppe of Inner Mongolia Plateau had much lower NDVI values (Fig. 1d, f). Such repeated ups and downs

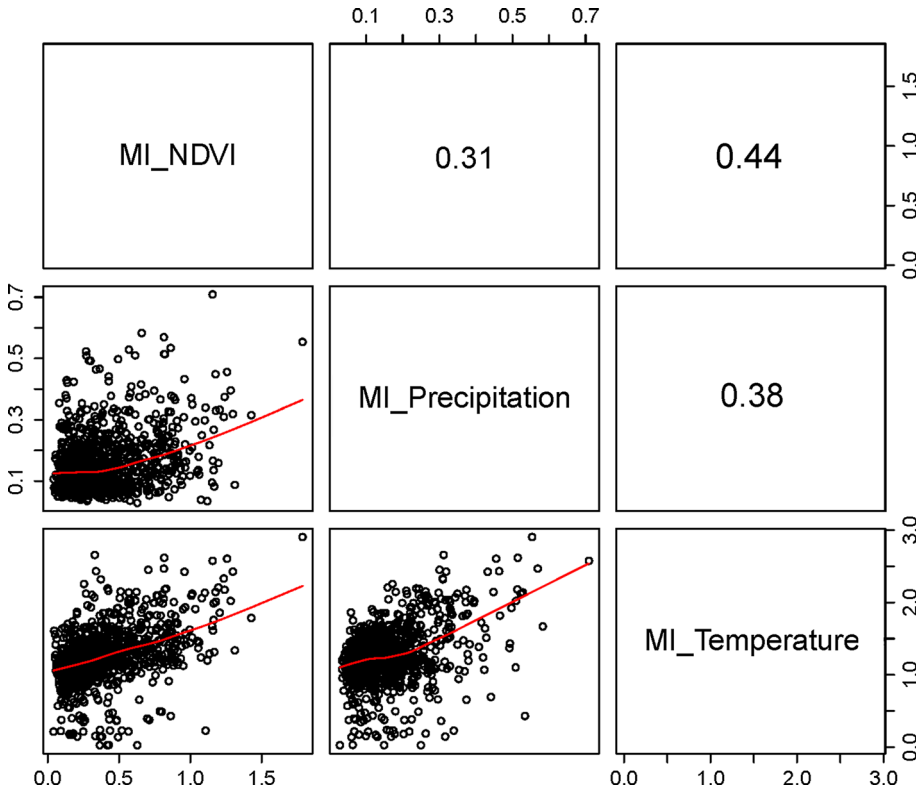

Fig. 5 Scatter graphs and Pearson correlation analysis of MI for NDVI, temperature, and precipitation time series. *Scatter graphs with the smooth lines* are on the *lower panels*, and *Pearson correlation coefficients* on the *upper panels*. We chose 1,000 random samples as a reference due to the very large whole dataset

caused a very poor degree of model fitting ($R^2 = 0.018$) (Table 4). This result implicitly reminds us that consideration of local factors and circumstances is necessary while doing global analyses.

Climate similarity and distance effect on vegetation dynamics similarity

The results of the Pearson correlation analysis indicated that similarities of NDVI time series were correlated positively and significantly with similarities of temperature ($R = 0.44$) and precipitation ($R = 0.31$) over the time series between any two stations (Fig. 5). In multiple regression analyses based on log-transformed geographical distance, MI values of temperature and precipitation time series explained 28 % of the MI values variation of NDVI time series for the whole 212,226 data points. When we partialled out log-transformed geographical distance, the MI values of temperature and precipitation remained highly correlated and significant ($R^2 = 0.260$, $P < 0.001$); when the effect of MI values of temperature and precipitation was removed, log-transformed geographical distance showed almost no correlation ($R^2 = 0.062$, $P < 0.001$).

However, the results from multiple regression analyses on the selected stations suggested that the numerical value of correlation coefficient and percentage of shared component explaining the similarity of NDVI time series were closely related to sampling directions. For station 54511, log-transformed geographical distance, MI of temperature and precipitation time series explained 58.7 % of the MI values variation of NDVI along latitude sampling belts. When we partialled out geographical distance, the MI values of temperature and precipitation remained highly correlated and significant ($R^2 = 0.574$, $P < 0.001$). While geographical distance on its own accounted for 40.8 % of the explained variation; MI of temperature explained on its own 56.5 %; and MI of precipitation explained on its own 44.3 % of the MI of NDVI variation. By contrast, on the longitude sampling belts, the three variables included explained 75.9 % of the total variation of MI of NDVI in the regression model ($P < 0.001$), and MI values of temperature and precipitation remained highly correlated and significant ($R^2 = 0.754$, $P < 0.001$) without geographical distance as explanatory variable.

Discussion

The results showed that all station pairs shared some similarity in the processes of climate variation and vegetation dynamics, conformed to the first statement in the "First Law of Geography"—"everything is related to everything else," which denotes explicit spatial dependence. This result is helpful in understanding the

synchronism and teleconnections in climate change. As the second statement of the "First Law of Geography" expresses, "near things are more related than distant things," distance played an important role in the relationships between "everything" and "everything else". The MI values between the selected stations and the other stations showed a gradual decrease with the increase of distance (Fig. 2), and the plots of MI versus distance showed a non-linear relationship. The results also suggested that the MI between two stations attenuates slowly down as the distance between the two stations increases. We simultaneously observed that the more steep the decay of MI in NDVI, temperature, and precipitation series from 0 to 500 km, the more gradual decline appeared in each series between 500 and 1,500 km, and a slight decline appeared between 1,500 km and 4,500 km. The rapid decay of MI at short distances suggested that strong dependence of variation only occurred at the local spatial scale. The idea of spatial similarity has been widely used in the field of geostatistics, especially in the analysis of spatial autocorrelation. Carrying a connotation of the results of this study, the results promotion, scaling, and spatial interpolation must be handled sensitively in future works.

Comparing the MI values of the three indexes in each station, MI of the temperature series at a given distance was at least two times higher than MI of the NDVI series and three times higher than MI of the precipitation series. Furthermore, as distance increased, the multiple rose gradually. Probably because temperature is highly determined by solar radiation, the variation of temperature was more steady and predictable. Compared to temperature, precipitation is more of a territorial characteristic. In addition to the impaction of land and sea distribution, local and mesoscale landforms also play important roles in variation of precipitation. Therefore, the precipitation series had significantly lower MI values. Additionally, distribution patterns and process of vegetation dynamics are mainly affected by hydrothermal conditions. Thus, MI values of the NDVI series were numerically between MI values of the temperature and precipitation series. Briefly speaking, different indexes had different MI value ranges and decay ratios due to various influential factors. The results imply that the temperature-related results obtained from the sampling points could represent larger regions than precipitation-related and vegetation-related results. Accordingly, we need to be more careful when generalizing the dry-wet variation from the sampling points to broader regions. In this context, further study is needed before reaching a definitive conclusion.

Several studies have revealed typically logarithmic distance-decay relationships between plant community similarity and distance (Tuomisto et al. 2003; Gilbert and Lechowicz 2004; Palmer 2005; Dornelas et al. 2006; Soininen et al. 2007), which provided support for a neutral theory of biogeography. In a recent analysis, Astorga et al. (2011) studied the community similarity of stream diatoms, macroinvertebrates, and bryophytes across the same set of sites in relation to distance and showed that the relationship was best approximated by a logarithmic model in each case, suggesting that patterns between macro- and microorganisms are not fundamentally different. In this paper, our findings show that the distance-decay relationship between the variation of climate elements and vegetation cover and distance is best approximated by a logarithmic model as well (Fig. 3; Table 4). Furthermore, natural community distribution, species assemblages, and biodiversity are directly impacted by regional climatic conditions. For instance, climax community, a basic concept in ecology, is defined in relation to regional climate. Thus, community similarity is related to climate similarity, including the climate variation similarity. Therefore, our results are of potential usefulness to the study of community similarity and the neutral theory of biogeography.

Distance-decay spatial models are based on the hypothesis that similarity between locations declines with distance even if the environment is completely homogeneous (Soininen et al. 2007). However, there is no completely homogeneous region in the real world. A study by Duque et al. (2009) showed that geographical distances alone accounted for 12 % of variation in floristic similarities, while both geographical distances and geology explained 64 % of the total variation in multiple regression analyses. Furthermore, the distance decay almost disappeared after removing environmental heterogeneity at fine scale. In this study, the decay was not smooth or homogeneous at large scale. For instance, Sichuan Basin (in Sichuan Province), Qaidam Basin (in Qinghai Province), Qinling Mountain area, and the areas along Huai River were low MI anomaly zones in the spatial patterns of MI values, especially in NDVI and temperature (Fig. 2). It signified that the variance of MI cannot be ascribed only to distance, which should be identical in every region. Distance decay alone was insufficient. The spatial heterogeneity of environmental factors, such as terrain mutations (Fig. 1), may be one reason for the non-stationary of decay. In the future, the vertical zonality and other combined effects of environment and geographical distances should be taken into consideration as part of explanations on similarity in climate variation and vegetation dynamics.

Conclusions

This study illustrates the strength of the distance-decay relationship within variations of climate and vegetation, and quantifies the relationship. The results suggest that

variations of climate and vegetation represent spatial dependence and obey the "First Law of Geography," and the distance-decay relationship is non-linear. Temperature, precipitation, and NDVI time series had different MI value ranges and distance-decay ratios due to various influential factors. The logarithmic distance-decay relationships are of potential usefulness to the study of community similarity and the neutral theory of biogeography. Besides distance, other combined effects of environment and topography should be taken into consideration as part of explanations on similarity in climate variation and vegetation dynamics. Our research provides an approach for analyzing spatial patterns in relation to dependence and synchronization that may inform future studies aiming to understand the distribution and spatial relationship of climate and vegetation change.

Acknowledgments This study was financially supported by grants from the National Natural Science Foundation of China (NSFC, Nos. 41330747 and 41130534) and China Postdoctoral Science Foundation funded project (2014M560014). The authors are grateful to the anonymous reviewers for offering valuable suggestions to improve the manuscript.

References

Astorga A, Oksanen J, Luoto M, Soininen J, Virtanen R, Muotka T (2011) Distance decay of similarity in freshwater communities: do macro-and microorganisms follow the same rules? Global Ecol Biogeogr 21(3):365–375

Baigorria GA, Jones JW (2010) GiST: a stochastic model for generating SPATIALLY and temporally correlated daily rainfall data. J Clim 23(22):5990–6008. doi:10.1175/2010jcli3537.1

Baigorria GA, Jones JW, O'Brien JJ (2007) Understanding rainfall spatial variability in southeast USA at different timescales. Int J Climatol 27(6):749–760. doi:10.1002/Joc.1435

Baselga A (2007) Disentangling distance decay of similarity from richness gradients: response to Soininen et al. 2007. Ecography 30:838–841

Bjorholm S, Svenning JC, Skov F, Balslev H (2008) To what extent does Tobler's 1st law of geography apply to macroecology? A case study using American palms (Arecaceae). BMC Ecol 8(1):11

Brown ME, Pinzon JE, Didan K, Morisette JT, Tucker CJ (2006) Evaluation of the consistency of long-term NDVI time series derived from AVHRR, SPOT-vegetation, SeaWiFS, MODIS, and Landsat ETM + sensors. Geosci Remote Sens IEEE Trans 44(7):1787–1793. doi:10.1109/TGRS.2005.860205

Chen WR, Henebry GM (2010) Spatio-spectral heterogeneity analysis using EO-1 Hyperion imagery. Comput Geosci UK 36(2):167–170. doi:10.1016/j.cageo.2009.05.005

Chen F, Yuan Y, Wen W, Yu S, Fan Z, Zhang R, Zhang T, Shang H (2012) Tree-ring-based reconstruction of precipitation in the Changling Mountains, China, since AD 1691. Int J Biometeorol 56(4):765–774

Cody ML (1975) Towards a theory of continental species diversities: bird distributions over Mediterranean habitat gradients. Ecol Evol Communities 214:257

Costantini ML, Zaccarelli N, Mandrone S, Rossi D, Calizza E, Rossi L (2012) NDVI spatial pattern and the potential fragility of mixed forested areas in volcanic lake watersheds. Forest Ecol Manag 285:133–141. doi:10.1016/j.foreco.2012.08.029

Cover TM, Thomas JA (2006) Elements of information theory, 2nd edn. Wiley-interscience, New York

Cressie N (1993) Statistics for spatial data. Wiley, New York

Davies RG, Orme CDL, Storch D, Olson VA, Thomas GH, Ross SG, Ding TS, Rasmussen PC, Bennett PM, Owens IPF (2007) Topography, energy and the global distribution of bird species richness. Proc R Soc B Biol Sci 274(1614):1189–1197

Domroes M, Ranatunge E (1993) Analysis of inter-station daily rainfall correlation during the southwest monsoon in the wet zone of Sri-Lanka. Geogr Ann A 75(3):137–148

Dornelas M, Connolly SR, Hughes TP (2006) Coral reef diversity refutes the neutral theory of biodiversity. Nature 440(7080): 80–82

Duque A, Phillips JF, von Hildebrand P et al (2009) Distance decay of tree species similarity in protected areas on terra firme forests in Colombian Amazonia. Biotropica 41:599–607

Evans KL, James NA, Gaston KJ (2006) Abundance, species richness and energy availability in the North American avifauna. Global Ecol Biogeogr 15(4):372–385

Geerken R, Zaitchik B, Evans JP (2005) Classifying rangeland vegetation type and coverage from NDVI time series using Fourier Filtered Cycle Similarity. Int J Remote Sens 26(24):5535–5554. doi:10.1080/01431160500300297

Gilbert B, Lechowicz MJ (2004) Neutrality, niches, and dispersal in a temperate forest understory. Proc Natl Acad Sci USA 101(20):7651–7656. doi:10.1073/pnas.0400814101

Gurgel HC, Ferreira NJ (2003) Annual and interannual variability of NDVI in Brazil and its connections with climate. Int J Remote Sens 24(18):3595–3609. doi:10.1080/0143116021000053788

Hofstra N, New M (2009) Spatial variability in correlation decay distance and influence on angular-distance weighting interpolation of daily precipitation over Europe. Int J Climatol 29(12):1872–1880. doi:10.1002/Joc.1819

Jarlan L, Mangiarotti S, Mougin E, Mazzega P, Hiernaux P, Le Dantec V (2008) Assimilation of SPOT/VEGETATION NDVI data into a sahelian vegetation dynamics model. Remote Sens Environ 112(4):1381–1394. doi:10.1016/j.rse.2007.02.041

Kadmon R, Pulliam HR (1993) Island biogeography: effect of geographical isolation on species composition. Ecology 74(4): 978–981

Kerr JT, Ostrovsky M (2003) From space to species: ecological applications for remote sensing. Trends Ecol Evol 18(6):299–305

Kraskov A, Stögbauer H, Grassberger P (2004) Estimating mutual information. Phys Rev E 69(6):066138

Legendre P, Legendre L (1998) Numerical ecology, 2nd English edn. Elsevier Science, Amsterdam

Lhermitte S, Verbesselt J, Jonckheere I, Nackaerts K, van Aardt JAN, Verstraeten WW, Coppin P (2008) Hierarchical image segmentation based on similarity of NDVI time series. Remote Sens Environ 112(2):506–521. doi:10.1016/j.rse.2007.05.018

Lhermitte S, Verbesselt J, Verstraeten WW, Coppin P (2011) A comparison of time series similarity measures for classification and change detection of ecosystem dynamics. Remote Sens Environ 115(12):3129–3152. doi:10.1016/j.rse.2011.06.020

Li SC, Zhao ZQ, Wang Y, Wang YL (2011) Identifying spatial patterns of synchronization between NDVI and climatic determinants using joint recurrence plots. Environ Earth Sci 64:851–859

Lichstein JW (2007) Multiple regression on distance matrices: a multivariate spatial analysis tool. Plant Ecol 188(2):117–131

Lobo A, Maisongrande P (2008) Searching for trends of change through exploratory data analysis of time series of remotely sensed images of SW Europe and NW Africa. Int J Remote Sens 29(17–18):5237–5245. doi:10.1080/01431160802036441

Mantel NA (1967) The detection of disease clustering and a generalized regression approach. Cancer Res 27:209–220
Martinez B, Cassiraga E, Camacho F, Garcia-Haro J (2010) Geostatistics for mapping leaf area index over a cropland landscape: efficiency sampling assessment. Remote Sens Basel 2(11):2584–2606. doi:10.3390/Rs2112584
Maselli F, Chiesi M (2006) Integration of multi-source NDVI data for the estimation of Mediterranean forest productivity. Int J Remote Sens 27(1):55–72
Millward AA, Kraft CE (2004) Physical influences of landscape on a large-extent ecological disturbance: the northeastern North American ice storm of 1998. Landsc Ecol 19(1):99–111
Morlon H, Chuyong G, Condit R, Hubbell S, Kenfack D, Thomas D, Valencia R, Green JL (2008) A general framework for the distance-decay of similarity in ecological communities. Ecol Lett 11(9):904–917
Myneni R, Tucker C, Asrar G, Keeling C (1998) Interannual variations in satellite-sensed vegetation index data from 1981 to 1991. J Geophys Res 103(D6):6145–6160
Nekola JC, White PS (1999) The distance decay of similarity in biogeography and ecology. J Biogeogr 26(4):867–878
Palmer MW (2005) Distance decay in an old-growth neotropical forest. J Veg Sci 16:161–166
Prates-Clark CD, Saatchi SS, Agosti D (2008) Predicting geographical distribution models of high-value timber trees in the Amazon Basin using remotely sensed data. Ecol Model 211(3–4):309–323. doi:10.1016/j.ecolmodel.2007.09.024
Shannon CE, Weaver W (1949) The mathematical theory of communication (Urbana, IL). Univ Ill Press 19(7):1
Soininen J, McDonald R, Hillebrand H (2007) The distance decay of similarity in ecological communities. Ecography 30(1):3–12
Sui DZ (2004) Tobler's first law of geography: a big idea for a small world? Ann Assoc Am Geogr 94(2):269–277
Tobler WR (1970) A computer movie simulating urban growth in the Detroit region. Econ Geogr 46:234–240
Tuomisto H, Ruokolainen K, Yli-Halla M (2003) Dispersal, environment, and floristic variation of western Amazonian forests. Science 299(5604):241–244. doi:10.1126/science.1078037
Viedma O, Torres I, Perez B, Moreno JM (2012) Modeling plant species richness using reflectance and texture data derived from QuickBird in a recently burned area of Central Spain. Remote Sens Environ 119:208–221. doi:10.1016/j.rse.2011.12.024
Vuilleumier F (1970) Insular biogeography in continental regions. I. The northern Andes of South America. Am Nat 104(938):373–388
Walsh SJ, Crawford TW, Welsh WF, Crews-Meyer KA (2001) A multiscale analysis of LULC and NDVI variation in Nang Rong district, northeast Thailand. Agr Ecosyst Environ 85(1–3):47–64
White MA, De Beurs KM, Didan K, Inouye DW, Richardson AD, Jensen OP, O'Keefe J, Zhang G, Nemani RR, Van Leeuwen WJD, Brown JF, De Wit A, Schaepman M, Lin X, Dettinger M, Bailey AS, Kimball J, Schwartz MD, Baldocchi DD, Lee JT, Lauenroth WK (2009) Intercomparison, interpretation, and assessment of spring phenology in North America estimated from remote sensing for 1982–2006. Glob Change Biol 15(10):2335–2359. doi:10.1111/j.1365-2486.2009.01910.x
Whittaker RH (1975) Communities and ecosystems. MacMillan Publishing, New York
Zhang X, Hu Y, Zhuang D, Qi Y (2009) The spatial pattern and differentiation of NDVI in Mongolia Plateau. Geogr Res Aust 1:002
Zhao ZQ, Gao JB, Wang YL, Liu JG, Li SC (2014) Exploring spatially variable relationships between NDVI and climatic factors in a transition zone using geographically weighted regression. Theoret Appl Climatol. doi:10.1007/s00704-014-1188-x